Structural Aspects of Optical Resolutions. Optical Resolution of (*R,S*)-Mandelic Acid. DSC and X-ray Studies of the Diastereoisomeric Salts

Mária Acs,*[a] Elisabeth Novotny-Bregger,[b] Kálmán Simon[c] and Gyula Argay[c]
[a] *Department of General and Analytical Chemistry, Technical Univ., Budapest, POB 91, H-1521, Hungary*
[b] *Institut für organische Chemie, ETH-Zürich, Zürich Universitätstrasse 16, CH-8092, Switzerland*
[c] *Central Research Institute for Chemistry of the Hungarian Academy of Sciences, Budapest, POB 17, H-1525 Hungary*

The diastereoisomeric salt pair formed during the resolution of mandelic acid (MA) using (*R*)-2-*tert*-butyl-3-methylimidazolidin-4-one (BMI) has been studied by DSC and X-ray crystallographic methods. Both diastereoisomers crystallize in a monoclinic system with space group $P2_1$; unit cell parameters for the less soluble *R–R* isomer: $a = 11.484(1)$, $b = 6.027(1)$, $c = 11.951(1)$ Å, $\beta = 98.77(1)°$, $V = 817.5(3)$ Å^3; for the more soluble *R–S* diastereoisomer $a = 11.170(1)$, $b = 5.975(1)$, $c = 13.327(1)$ Å, $\beta = 111.95(1)°$, $V = 825.0(3)$ Å^3. The structures were solved by direct methods and refined to a final *R* value of 0.044 and 0.057, respectively.

With the growing interest in producing enantiopure substances, more attention is being paid to the problems of resolution. One of the most frequent means of obtaining enantiopure compounds on an industrial scale is still resolution *via* diastereoisomeric salts. The main problems of this type of enantiomer separation are the selection of the best resolving agent, and solvent, and the prediction of the efficiency of the resolution and the configuration of the enantiomer present in excess in the precipitating diastereoisomeric salt.[1] To find possible answers to these questions several working hypotheses based mainly on empirical experiences have been reported.[2] Among these questions, some are related to the structures of the diastereoisomeric salt pairs, *i.e.* the larger the differences in the solid state, the more efficient resolution can be expected. Systematic structure investigations of salts including the most widely used resolving agents[3,4] [(2*R*,3*R*)-tartaric acid,[5] brucine,[6] strychnine,[7] α-methylbenzylamine[8]] have revealed that common features characterize the solid state arrangement of the corresponding salt families. Unfortunately, relatively few structure analyses of pairs of diastereoisomeric salts are available. Among them the acidic tartrates have been exhaustively studied,[5] but their use as resolving agents is sometimes inconvenient and handicapped by the fact that only the (2*R*,3*R*) isomer is available at a reasonable price. Among the synthetic resolving agents, mandelic acid gained an important role,[4] as both enantiomers are sold at nearly equal price. Therefore, diastereoisomeric mandelate salts are worth investigating. In X-ray studies, mandelic acid enantiomers are the favoured internal reference (counter)ions for determining the absolute configuration of new drug molecules, but practically no diastereoisomeric mandelic salt pairs have been analysed in detail. (The crystal structure of ephedrine and pseudoephedrine mandelates were described in a PhD thesis.[9]) Our aim was to perform a detailed analysis of a diastereoisomeric mandelate pair to compare the structures with each other and with known structures, and to reveal the relationship, if any, between differences in structure and thermal stability on the one hand and the efficiency of the given resolution on the other hand. As model compounds, diastereoisomeric 2-*tert*-butyl-3-methyl-4-oxoimidazolidinium mandelates were chosen. *N'*-Acylated derivatives of BMI are versatile key intermediates in the synthesis of specifically substituted amino acids.[10] The diastereoisomeric salts are referred to as BMI–*S*-MA and BMI–*R*-MA corresponding to the characteristic initials of the IUPAC names for the individual compounds (Mandelic Acid and 2-*tert*-Butyl-3-Methyl-1,3-Imidazolidin-4-one). Racemic BMI is successfully resolvable with optically active mandelic acid isomers,[10] while racemic mandelic acid can be resolved by using *R*- (or *S*-)-BMI base (Scheme 1). The resolution occurs with high efficiency (EC >0.6) in both directions. (The efficiency = enantiomer content: EC is defined as the product of the optical purity and the chemical yield of the precipitating diastereoisomeric salt.[11])

Results and Discussion

Binary Phase Diagram of the Diastereoisomeric Mandelates.— In order to gain deeper insight into the general mechanism of chiral discrimination (or resolution in our case) not only the detailed molecular and crystal structure studies of the diastereoisomeric salts are needed, but their 'behaviour' during the course of the crystallization is also of interest, *i.e.* their mixture also had to be investigated. In those cases where no solvate retention or polymorphism occurs, the binary phase diagram describes well the main types of interaction between the chemical entities taking part in the resolution procedure. The binary phase diagram can also provide information about the influence of kinetic and thermodynamic factors on the efficiency of the resolution. In those cases where the mechanical mixture, *i.e.* conglomerate, of the diastereoisomeric salts precipitates from the reaction mixture, the efficiency, EC, of the resolution at thermodynamic equilibrium is determined by the eutectic composition.[12] The maximum EC can be calculated from eqn. (1) where x_e represents the molar fraction of the less

$$EC = (1 - 2x_e)/(1 - x_e)$$

soluble diastereoisomeric salt in the eutectic.[13] If the experimentally obtained enantiomer content is in good agreement with the calculated one, kinetic control plays a negligible role in the resolution. Thus constructing the binary phase diagram, we calculated the theoretical value of EC knowing the eutectic composition ($x_e = 0.13$, and $EC_{calc} = 0.85$) and compared it to the experimental value ($EC_{exp} = 0.91$). The calculated and the experimentally obtained values are close enough to show that our assumption of conglomerate formation was correct and that the resolution is a thermodynamically controlled process.

The binary phase diagram was calculated with the Schröder van Laar equation[14] (Fig. 1, continuous line) and the

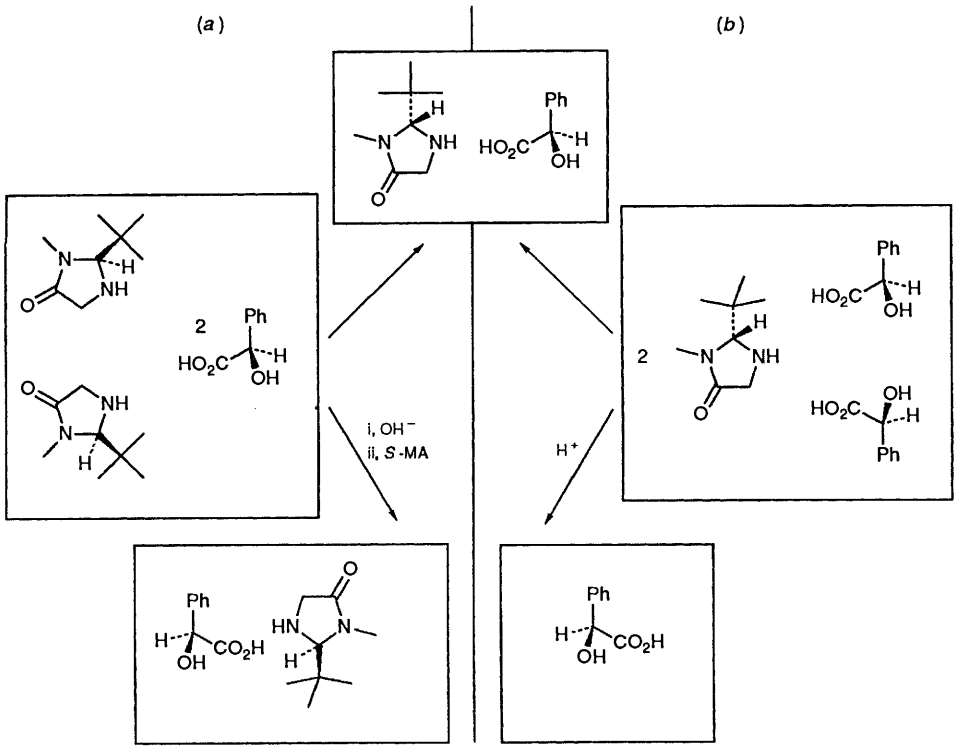

Scheme 1 (*a*) BMI enantiomers reacted with equivalent amount of (*R*)-mandelic acid in acetone, produce diastereoisomeric salts in equal amounts. The less soluble *R*-BMI–*R*-mandelate precipitates (yield: 60%). After evaporating the solvent the *S*-base is liberated and the non-racemic mixture is allowed to react with (*S*)-mandelic acid equivalent to the *S*-base present in the mixture. As the two experiments are in mirror-image relationship, enantiopure *S*-base–*S*-acid salt crystallizes (yield: *ca.* 40%). (*b*) The reciprocal resolution produces both mandelic acid isomers in one resolution step, using one equivalent of *R*-BMI. The efficiency of the separation amounts to EC = 0.9 for both isomers.

Table 1 Thermal data of different diastereoisomeric compositions

	Melting point/K					
R/*S*	Calculated[a]		Measured		Heat of fusion/ kcal mol^{-1} [b]	x_{eu}
1 0	—	—	—	391	11.88	Calculated[a]
7 3	348	382	350	384	—	0.15
1 1	349	374	349	377	—	
2 8	348	354	349	352	—	Measured
0 1	—	—	—	352	6.98	0.13

[a] Calculated with the aid of Schröder van Laar equations. [b] 1 cal = 4.184 J.

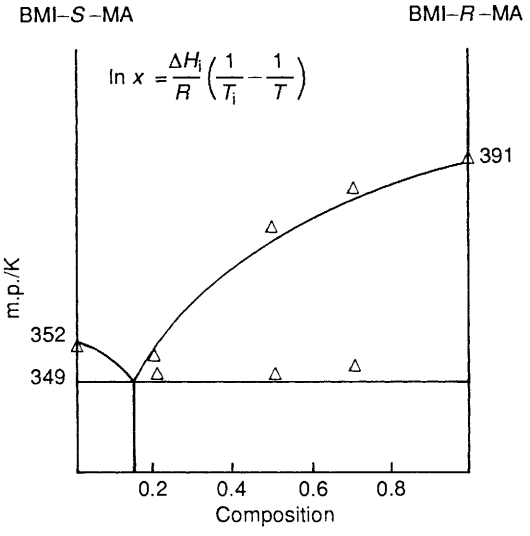

Fig. 1 Melting point–composition (binary phase) diagram of the diastereoisomeric BMI–mandelates calculated by the Schröder van Laar equation (measured data: Δ)

calculations checked by comparison with the observed melting points of different stereoisomeric mixtures (Table 1, Fig. 1). Heats of fusion and melting points were measured by differential scanning calorimetry (DSC).

X-Ray Studies of the Diastereoisomeric Mandelates.—The diastereoisomeric salt pair was prepared from the second resolution procedure mentioned above and the obtained *R*-BMI–*R*-mandelate (BMI–*R*-MA) and *R*-BMI–*S*-mandelate (BMI–*S*-MA) were subjected to complex thermoanalytical and single crystal X-ray studies. Crystal data and details of structure solution and refinement are compiled in Table 2. PLUTO diagrams of the ion pairs of BMI–*R*-MA and BMI–*S*-MA are shown in Figs. 2 and 3, respectively. Selected torsion angles and hydrogen bonds are given in Tables 3 and 4, respectively.

Conformation of the counterions. Mandelate anions exhibit enantiomeric but otherwise similar conformations: the torsion angles O(19)–C(18)–C(12)–C(17) are −45 and +45°, respectively. C–O bond lengths in the carboxyl groups are nearly the same, indicating comparable participation in salt bridges. The C–O bond lengths in the carboxyl group of mandelic acid are 1.314 Å and 1.211 Å.[19] The two C–O bond lengths in the more stable salt (BMI–*R*-MA) are very similar [1.263(4) Å and 1.248(5) Å] while in the more soluble salt (BMI–*S*-MA), the difference is somewhat more pronounced [1.249(5) Å and 1.276(9) Å].

Corresponding to the homochirality of the rigid imidazolidinone ring, BMI cations in the diastereoisomeric mandelates are characterized by nearly identical conformations. As expected the 1,3-imidazolidine ring shows an envelope conformation with the C(2) atom above the plane of the rest of the ring. The

Table 2 Crystal, structure solution and refinement data of the diastereoisomeric BMI–mandelates

	BMI-*R*-MA	BMI-*S*-MA
Empirical formula	$C_{16}H_{24}N_2O_4$	$C_{16}H_{24}N_2O_4$
Colour, habit	transparent needles	
Crystal size	0.15 × 0.35 × 0.80	0.05 × 0.2 × 0.4
Crystal system	monoclinic	monoclinic
Space group	$P2_1$	$P2_1$
a (Å)	11.484(1)	11.170(1)
b (Å)	6.027(1)	5.975(1)
c (Å)	11.951(1)	13.327(1)
β (°)	98.77(1)	111.95(1)
Volume (Å^3)	817.5(3)	825.0(3)
Z	2	2
Formula weight	308.38	308.38
Density (g/cm^3, calc.)	1.253	1.242
Absorption coef. (cm^{-1})	7.011	0.835
F(000)	332	332
Solution	direct methods	
	MULTAN 78[a]	SHELX 86[b]
Radiation	Cu-Kα (λ = 1.5418 Å)	Mo-Kα (λ = 0.7107 Å)
Temperature (K)	298	298
Monochromator	graphite crystal	
2θ Range (°)	3.0–150	3.0–50
Independent reflections	1817	1574
Observed reflections	1728 $I > 3\sigma(I)$	1173 $I > 3\sigma(I)$
Absorption correction	semi-empirical	no
Min/max abs. correction	0741/1.333	—
Final $R_{unweighted}$	0.044	0.057
	F magnitudes in least squares refinements	
No. of variables	295	199
	H-atoms refined isotropically	H-19 taken from diff. Fourier map. All other H-atoms were generated
$(\Delta\rho)_{max}$(e/Å^3)	0.2	0.3
Decay correction	no decay during the measurements	
$(\Delta/\sigma)_{max}$	0.9	0.5
Method of mes. reflections	$\theta/2\theta$	$\theta/2\theta$
R_w	0.049	0.065
W	unit weight	

[a] P. Main, S. E. Hull, E. Lessinger, G. Germain, J. P. Declercq, M. M. Wolfson, MULTAN78. A System of Computer Programs for the Automatic Solution of Crystal Structures from X-ray diffraction Data. Universities of York (GB) and Louvain-la-Neuve (Belgium), 1978. [b] G. M. Sheldrick, SHELX86 a FORTAN-77 Program for the Solution of Crystal Structures from Diffraction Data, University of Göttingen (FRG) 1986.

amide nitrogen atom [N(3)] is trigonal (planar) so that the lone pair can be delocalized toward the carbonyl group. The *tert*-butyl group occupies the same relative position with respect to the nearly planar ring moiety. Relating the spatial arrangement of substituents at C(2) to the known absolute configuration of mandelic acid, the configuration of the resolving (−)-base {$[\alpha]_D = -24.2°$ (c 1 in acetone), $-92.1°$ (c 1 in MeOH) at room temperature} is derived to be *R*.

Hydrogen bonding system. The enantiomeric relationship between the anions results in the different number and strengths of the hydrogen bonds formed intra- and inter-molecularly. An intramolecular hydrogen bond is formed in the *R*-anion between the OH [O(19)] and the carbonyl oxygen [O(22)] of the carboxylic group forcing the groups approximately into the same plane [O(22)–C(20)–C(18)–O(19): 9.9°]. An interesting feature of *R*-MA is that besides the O(21) and O(22) acceptor atoms, O(19) also serves as an acceptor in the hydrogen bonding network (Table 4). In the *S*-isomer the O(22) atom acts as a double acceptor. H(19) is bifurcated and takes part in two relatively weak hydrogen bonds (Table 4). The presence of the

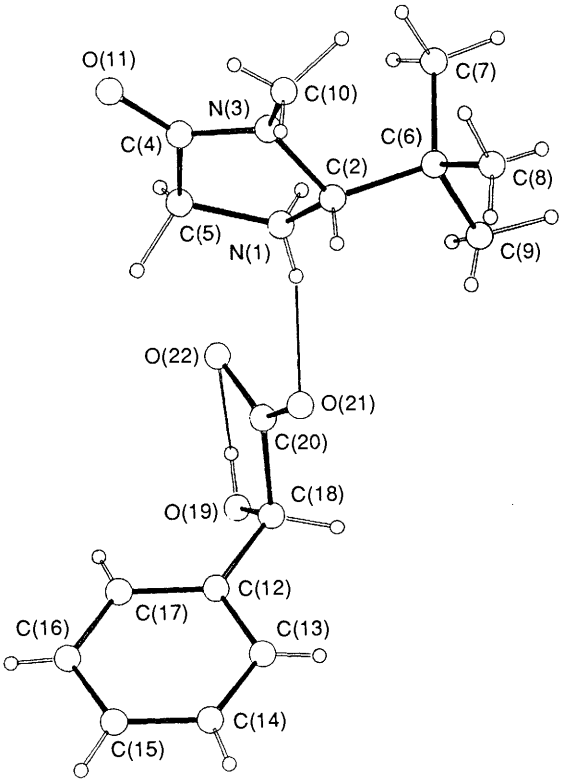

Fig. 2 PLUTO diagram of the ion pair of *R*-BMI–*R*-MA

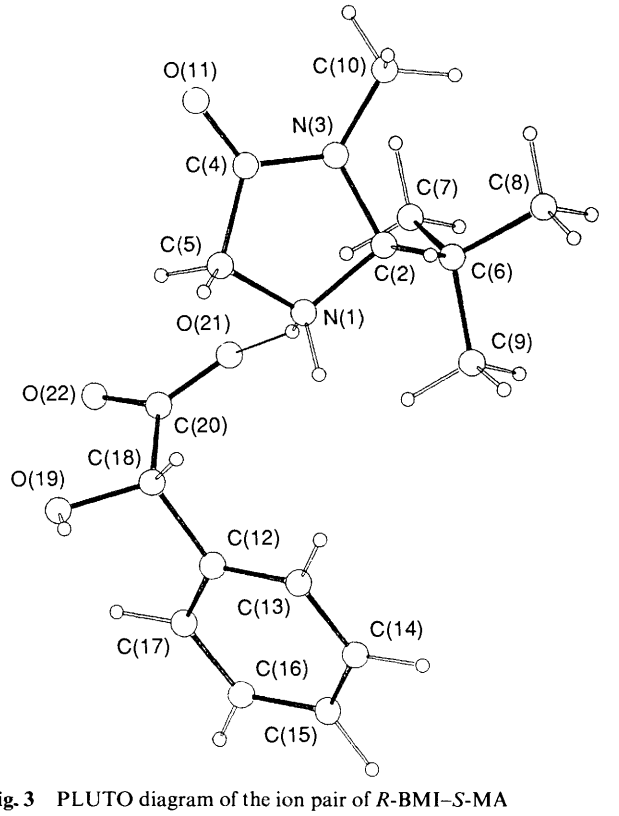

Fig. 3 PLUTO diagram of the ion pair of *R*-BMI–*S*-MA

internal O(19)–H(19) · · · O(22) bond in BMI–*R*-MA causes significant shifts in the ν_{OH} and $\nu_{C=O}$ IR bands relative to the corresponding data for BMI–*S*-MA (Table 5).

Interactions between counter ions. Salt bridges are formed between O(21) and N(1)–H(1b) atoms in both salts. In BMI–*R*-MA a second hydrogen bond occurs between the hydrogen attached to N(1) [H(1a)] and the alcoholic oxygen atom

Table 3 Torsion angles (deg) with e.s.d.s

	BMI-*R*-MA	BMI-*S*-MA
N(3)-C(4)-C(5)-N(1)	−7.1(4)	−2.2(8)
C(4)-N(3)-C(2)-N(1)	18.6(4)	19.8(8)
C(4)-C(5)-N(1)-C(2)	18.5(4)	14.4(8)
C(5)-N(1)-C(2)-N(3)	−22.3(4)	−20.4(8)
C(5)-C(4)-N(3)-C(2)	−7.5(4)	−11.7(8)
C(6)-C(2)-N(1)-C(5)	−148.8(6)	−145.1(9)
C(6)-C(2)-N(3)-C(4)	141.6(6)	141.0(10)
C(7)-C(6)-C(2)-N(1)	73.3(5)	73.6(7)
C(7)-C(6)-C(2)-N(3)	−44.4(5)	−42.3(8)
C(8)-C(6)-C(2)-N(1)	−164.8(6)	−164.8(10)
C(8)-C(6)-C(2)-N(3)	77.6(5)	79.3(8)
C(9)-C(6)-C(2)-N(1)	−46.6(5)	−47.5(7)
C(9)-C(6)-C(2)-N(3)	−164.3(6)	−163.3(7)
C(10)-N(3)-C(2)-N(1)	172.8(6)	175.0(10)
C(10)-N(3)-C(2)-C(6)	−64.2(6)	−63.0(12)
C(10)-N(3)-C(4)-C(5)	−162.2(7)	−166.9(13)
O(11)-C(4)-N(3)-C(2)	172.3(8)	166.4(14)
O(11)-C(4)-N(3)-C(10)	17.6(6)	11.2(12)
O(11)-C(4)-C(5)-N(1)	173.1(7)	179.7(13)
O(19)-C(18)-C(12)-C(13)	136.0(6)	−134.3(10)
O(19)-C(18)-C(12)-C(17)	−44.6(5)	44.9(9)
C(20)-C(18)-C(12)-C(13)	−105.0(6)	105.1(10)
C(20)-C(18)-C(12)-C(17)	74.5(6)	−74.7(10)
O(21)-C(20)-C(18)-C(12)	67.9(6)	−79.9(10)
O(21)-C(20)-C(18)-O(9)	−171.2(6)	160.3(11)
O(22)-C(20)-C(18)-C(19)	9.9(5)	−22.1(9)

Table 4 Hydrogen bonds in the diastereoisomeric mandelates

D-H···A (atoms involved)	Symmetry[a]	D-A/ Å	H-A/ Å	DHA/°
BMI-*R*-MA				
N(1)-H(1a)···O(19)	2	2.864(4)	1.95	165
N(1)-H(1b)···O(21)	1	2.584(3)	1.81	155
O(19)-H(19)···O(22)	1	2.542(4)	1.99	130
BMI-*S*-MA				
N(1)-H(1a)···O(22)	3	2.628(6)	1.57	166
N(1)-H(1b)···O(21)	1	2.776(6)	1.75	158
O(19)-H(19)···O(22)	4	2.805(6)	2.12	134
O(19)-H(19)···O(19)	4	3.081(6)	2.27	151

[a] Symmetry operations: 1: [x, y, z]; 2: [$-x, y - 0.5, 1 - z$]; 3: [$x, y + 1, z$]; 4: [$1 - x, y + 0.5, -z$].

Table 5 Characteristic differences in IR spectra of the diastereoisomeric mandelates (KBr pellets)

ν/cm^{-1}	BMI-*R*-MA	BMI-*S*-MA
ν_{OH}	3240[a]	3400[a]
$\nu_{=CH}$	3080–3060	3100–3060
$\nu_{C=O}$	1740[b]	1720[b]
ν_{amidel}	1680	1660
ν_{asCH_3}	1500–1400	1400–1300
β_{OH}	1240	1220
ν_{C-O}	1120–1000	1100–980
$\gamma_{OH(acid)}$	920	910
$\gamma_{=CH(monosubs)}$	780	800
$\nu_{C=C(monosubs)}$	670	650

[a] H-bridged alcoholic hydroxy. [b] H-bridged carbonyl/carboxyl group.

[O(19)] of the symmetry-related mandelic acid in the *R*-mandelate. Owing to the twofold screw axis in the crystal, these hydrogen bonds bind the asymmetric unit to two other asymmetric units, one above and one below (Fig. 4). This explains the relatively short *b* axis for the *R*-mandelate salt and leads to an infinite hydrogen bonding helix along the *b* axis. In BMI-*S*-MA the hydrogen atoms attached to N(1) are donated to the O(21) and O(22) atoms of translation-related mandelate anions above and below (Fig. 5) thus forming two infinite hydrogen bonding chains related by the 2_1 axis and interconnected by O(19)-H···O(22) and O(19)-H···O(19) hydrogen bonds.

Comparison of the crystal structures. Phenyl rings of mandelic acid and imidazolidine rings of the base are stacked along the *b* axis. The orientation of the phenyl rings relative to the *a,c*-plane is similar in the two structures, while that of the imidazolidine rings is different.

The helices mentioned above for BMI-*R*-MA are bound together by van der Waals interactions between the alkyl and aryl fragments of the molecules and dipole–dipole interactions between the carbonyl groups (Fig. 4). Interestingly, the less stable diastereoisomer (BMI-*S*-MA) lacks the helical arrangement of the hydrogen bonding system, and a continuous hydrogen bond chain can be traced between the mandelate anions along the *b* axis. The O(19)-H(19)···O(22) hydrogen bonds form a second infinite hydrogen bond chain.

Dipole–dipole interactions are established between the amide carbonyl groups of the symmetry-related cations [C(4)-O(11)···O(11)-C(4)] while *tert*-butyl groups are in close proximity to the corresponding symmetry-related *tert*-butyl fragments.

Common features of mandelic acid-containing structures. A bibliographic search of the Cambridge Crystallographic Data Base file (January 1991) using the 'MAND' string resulted in 40 hits. False hits, covalently substituted and complexed mandelic acid derivatives were sorted out by hand. The set was completed by four diastereoisomeric salt structures taken from a dissertation abstract,[9] the structures reported in this paper, and the mandelate salt of a recently published methylpyrrolidine derivative.[15] In this way 24 different mandelic acid fragments were identified, three of them characterizing the free acids: racemic (DLMAND)* and *S*-isomer (FEGHAA, this latter with two independent molecules in the asymmetric unit). In three more cases the asymmetric unit also consisted of two independent molecules (FEMLUE, FOYZUO and MPY-*S*-MA).

To make the conformational analysis consistent, atoms C(13) and C(17) of the phenyl ring and atoms O(21) and O(22) of the carboxyl group were distinguished as follows. Atom C(17) was defined to have the smaller absolute value of the two O(19)-C(18)-C(12)-C_{ortho} torsional angles. Similarly, the smaller of the two torsion angles O(19)-C(18)-C(20)-$O_{carboxyl}$ was defined as O(19)-C(18)-C(20)-O(22). Table 6 lists the results. Only the bond lengths and angles of the carboxyl group seemed to be of interest. In the free acids (DLMAND, FEGHAA), the differences between the C-O and C-O(H) bonds are significant. The O-C-O bond angle is always larger than 120°. The conformation of the molecules across the two single bonds is defined by the C(17)-C(12)-C(18)-O(19) and O(19)-C(18)-C(20)-O(22) torsion angles. Comparing the *R*-enantiomers in all cases the C(17)-C(12)-C(18)-O(19) torsion angle is in the range of −85.2° to +26.2°, while the O(19)-C(18)-C(20)-O(22) torsion angle is in the range of −5.6 to +39.8 degrees. According to our definition extreme values for both torsion angles would be ±90°.

The position of the phenyl group relative to the hydroxy group can change in a wider range than that of the hydroxy and carboxyl groups, probably owing to the possibility of intramolecular O-H···O hydrogen bonding.

For the *R*-enantiomer, the C(17)-C(12)-C(18)-O(19) torsion angle is biased towards negative values, while the O(19)-C(18)-C(20)-O(22) torsion angle is biased, to a smaller degree, towards positive values.

* Abbreviations are defined in Table 6.

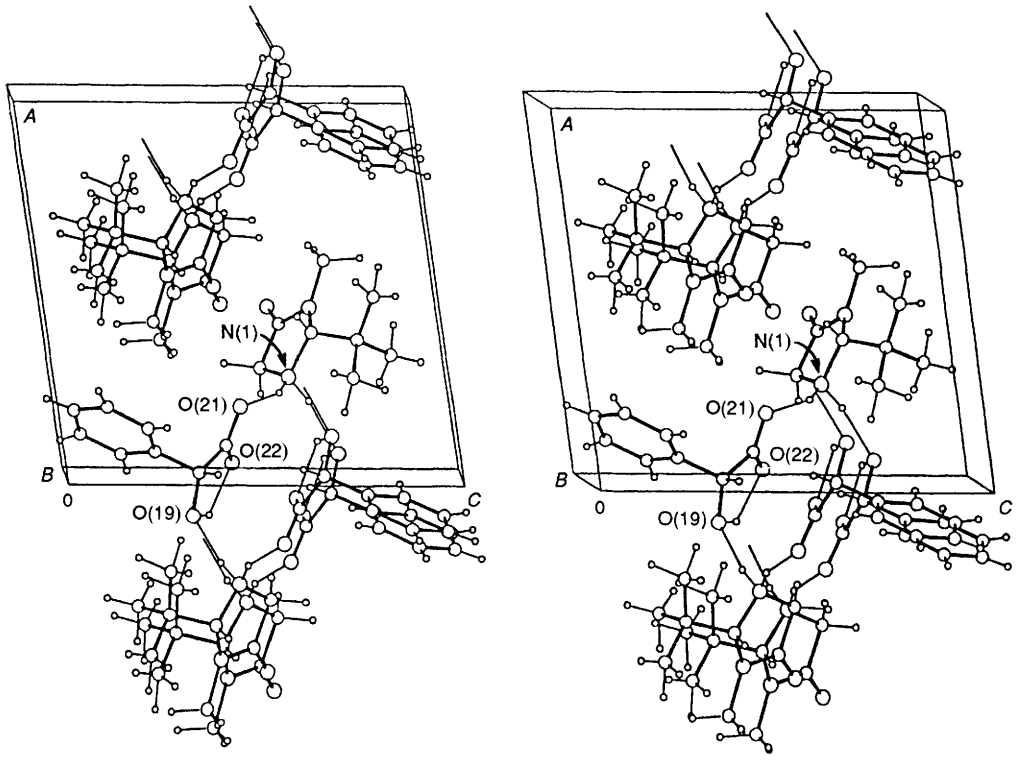

Fig. 4 Packing diagram of *R*-BMI–*R*-MA with the program PLUTO

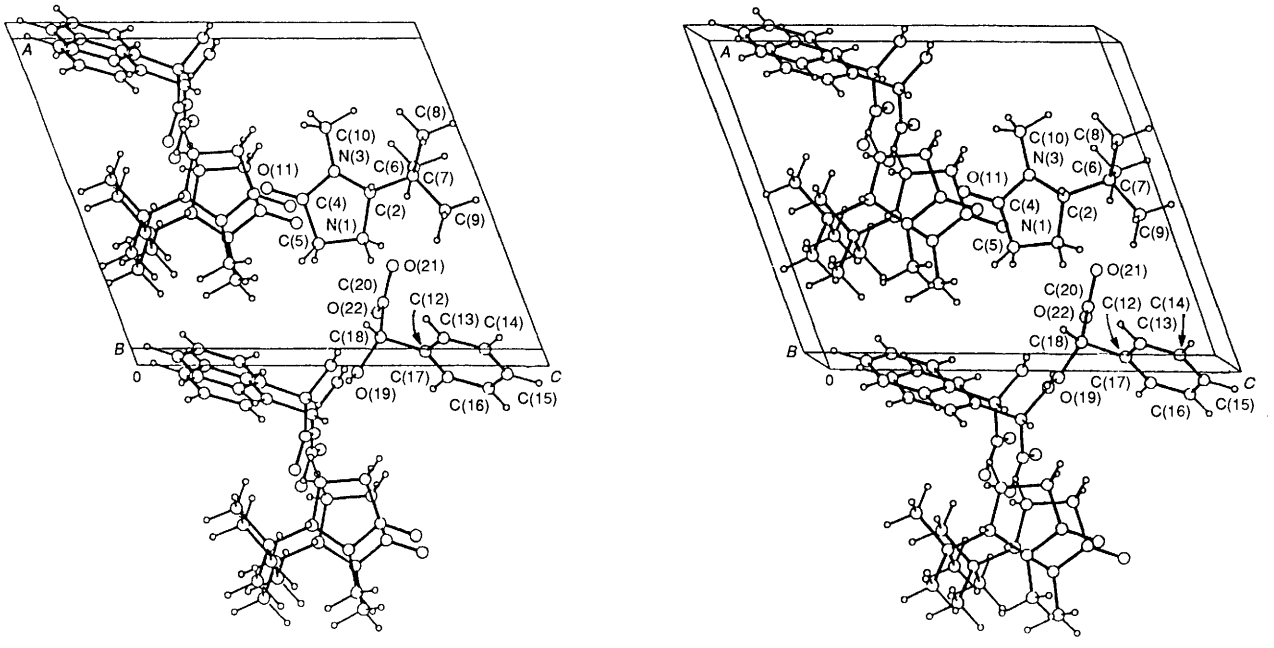

Fig. 5 Packing diagram of *R*-BMI–*S*-MA with the program PLUTO

Experimental

Thermoanalytic measurements were carried out using a Mettler FP84 DSC apparatus, controlled by an FP800 unit. Optical rotations were measured on a Perkin-Elmer 241 polarimeter. IR spectra were recorded on a SPECORD-75. Crystallographic measurements were carried out on ENRAF-NONIUS CAD-4 diffractometers. All computations were performed with the E.N. SDP program package on a PDP-11 computer. Atomic coordinates are given in Tables 7 and 8. Anisotropic displacement parameters, bond lengths and angles and hydrogen atom co-ordinates have been deposited at the Cambridge Crystallographic Data Centre.*

Resolution of Mandelic Acid.—(R)-2-tert-*Butyl*-3-*methyl*-4-*oxoimidazolidinium* (R)-*mandelate*. Racemic mandelic acid (0.75 g, 0.005 mol) was dissolved in acetone (1.5 cm^3) at 25 °C. To the resulting clear solution, was added *R*-BMI (0.78 g) dissolved in acetone (0.65 cm^3). Precipitation of the BMI–*R*-MA commenced immediately, and was completed after 1 h standing at room temperature. The crystalline mass was filtered off, washed with cold acetone (0.75 g, 98% of the theoretical amount of BMI–*R*-MA). The pure diastereoisomeric salt was obtained by recrystal-

* For details of the deposition scheme see 'Instructions for Authors,' *J. Chem. Soc., Perkin Trans. 2*, 1992, issue 1.

Table 6 Comparison of the selected geometrical parameters[a] of different crystal structures, containing mandelic acid on the basis of a CSD search

Refcodes[b]	20–22	20–21	21–20–22	17–12–18–19	19–18–20–22	Space group	Configuration
BERVUP	1.226	1.248	127.2	−70.3	13.8	$P2_12_12_1$	*R*
BERWAW	1.220	1.238	130.6	−50.1	22.5	$P2_1$	*R*
DLMAND	1.211	1.294	123.7	−68.0	24.3	*Pbca*	*R*
DMPYRM	1.260	1.248	124.9	43.9	−23.1	*P*1	*S*
FAYBOW	1.273	1.230	127.4	22.9	−13.5	$P2_1$	*S*
FEGHAA A	1.199	1.301	126.3	31.9	−2.2	$P2_1$	*S*
FEGHAA B	1.200	1.304	125.8	79.4	1.2	$P2_1$	*S*
FEMLUE A	1.240	1.293	124.6	−46.2	35.1	$P2_1$	*R*
FEMLUE B	1.238	1.273	125.8	−9.7	18.7	$P2_1$	*R*
FOYZUO A	1.259	1.238	126.9	−11.4	36.7	*P*1	*R*
FOYZUO B	1.244	1.260	126.4	−32.1	18.2	*P*1	*R*
FUPBUN	1.247	1.246	126.8	−26.2	5.6	$P2_12_12_1$	*S*
KAMMOA	1.238	1.237	126.9	−34.8	10.3	$P2_1$	*R*
KECTOB	1.256	1.254	124.6	−22.4	−35.0	$P2_1$	*S*
PEAMAN	1.231	1.274	125.2	35.7	−11.5	$P2_12_12_1$	*S*
SAYPOX	1.256	1.248	127.4	−21.8	8.6	$P2_12_12_1$	*R*
DINKUG01	1.241	1.284	123.6	85.3	−12.4	*C*2	*S*
DINLAN01	1.231	1.251	126.8	−17.5	39.8	$P2_12_12_1$	*R*
GAJPIQ	1.246	1.233	127.8	−40.6	14.1	$P2_12_12_1$	*R*
GAJPOW	1.222	1.254	127.7	−42.4	11.0	$P2_12_12_1$	*R*
MPY-*S*-MA A	1.242	1.235	125.4	64.7	−16.8	$P2_12_12_1$	*S*
MPY-*S*-MA B	1.242	1.258	126.0	1.3	−34.8	$P2_12_12_1$	*S*
BMI-*S*-MA	1.276	1.249	124.6	44.9	−22.1	$P2_1$	*S*
BMI-*R*-MA	1.248	1.263	124.9	−44.6	9.9	$P2_1$	*R*

[a] Bond lengths in Å, angles in degrees. [b] BERVUP *threo-o*-bromomandelamidinium mandelate: J. Iball, J. N. Low, D. G. Neilson and C. H. Morgan, *Cryst. Struct. Commun.*, 1982, **11**, 349. BERWAW *erythro-o*-bromomandelamidinium mandelate: J. Iball, J. N. Low, D. G. Neilson and C. H. Morgan, *Cryst. Struct. Commun.*, 1982, **11**, 349. DLMAND DL-mandelic acid: T. S. Cameron and M. Duffin, *Cryst. Struct. Commun.*, 1974, **3**, 539. DMPYRM *trans*-(2*R*,5*R*)-2,5-dimethylpyrrolidinium (*S*)-mandelate: L.-K. Liu and R. E. Davis, *Acta Crystallogr. Sect. B*, 1980, **36**, 171. FAYBOW (+)-Biperidenium L(+)-mandelate: P. W. Codding, *Acta Crystallogr. Sect. B*, 1986, **42**, 632. FEGHAA *S*-(+)-mandelic acid: A. O. Patil, W. T. Pennington, I. C. Paul, D. Y. Curtin and C. E. Dykstra, *J. Am. Chem. Soc.*, 1987, **109**, 1529. FEMLUE (1*R*,4a*S*,5*R*,9b*S*)-(+)-1-methyl-5-phenyl-2,3,4,4a,5,9b-hexahydro-1-*H*-indeno[1,2-*b*]pyridine D(−)-mandelic acid: R. Kunstman, G. Gerhards, H. Kruse, M. Leven, E. F. Paulus, U. Schacht, K. Schmitt and P. U. Witte, *J. Med. Chem.*, 1987, **30**, 798. FOYZUO (1*S*,2*S*)-(+)-*trans*-2-pyrrolidinyl-*N*-methylcyclohexylammonium (*R*)-(−)-mandelate: B. DeCosta, C. George, R. B. Rothman, A. E. Jacobsen and K. C. Rice, *Fed. Eur. Biochem. Soc.*, 1987, **223**, 335. FUPBUN (+)-(4a*R*,8a*R*)-2-methyl-4-αβ-(3-methoxyphenyl)-1,2,3,4,4a,5,6,7,8,8 *ao*-decahydro isoquinolinium mandelate dihydrate: D. M. Zimmerman, B. E. Cantrell, J. K. Schwartzendruber, N. D. Jones, L. G. Mendelsohn, J. D. Leander and R. C. Nickander, *J. Med. Chem.*, 1988, **31**, 555. KAMMOA 1-[(*S*)-cyclohexyl-1-hydroxy-1-phenylbutyl]piperidinium (*R*)-mandelate: R. Tacke, C. Strohmann, S. Sarge, H. K. Cammenga, D. Schomburg, E. Mutschler and G. Lambrecht, *Liebigs Ann. Chem.*, 1989, 137. KECTOB [(−)-(3*R*,4*R*)-3-propylammonio]-6-methoxy-1-benzopyran-4-ol (*S*)-(+)-mandelate: H. A. DeWald, T. G. Heffner, J. C. Jaen, D. M. Lustgarten, A. T. McPhail, L. T. Meltzer, T. A. Pugsley and L. D. Wise, *J. Med. Chem.*, 1990, **33**, 445. PEAMAN 1-Phenylethylammonium mandelate ref. 8. SAYPOX (−)-(4a*R*,10a*R*)-*trans*-1,2,3,4,4a,5,10,10-*a*-octahydro-6-hydroxy-1-propylbenzo[*g*]quinolinium-(*R*)-(−)-mandelate: M. P. Seiler, R. Markstein, M. D. Walkinshaw and J. J. Boelsterli, *Mol. Pharmacol.*, 1989, **35**, 643. DINKUG01 (1*S*,2*R*-(+)-ephedrinium (*S*)-(+)-mandelate ref. 9. DINKLAN01 (1*S*,2*R*)-(+)-ephedrinium (*R*)-(−)-mandelate ref. 9. GAJPIQ (1*R*,2*R*-(−)-pseudoephedrinium (*R*)-(−)mandelate ref. 9. GAJPOW (1*S*,2*S*)-(+)-pseudoephedrinium (*R*)-(−)-mandelate ref. 9. MPY-*S*-MA *cis*-2-(1-hydroxy-1-methylethyl)-5-methylpyrrolidinium (*S*)-mandelate ref. 15.

Table 7 Fractional co-ordinates for BMI-*R*-MA with e.s.d.s in parentheses

Atom	*x*/a	*y*/b	*z*/c
N(1)	0.2843(2)	0.0000	0.5960(2)
C(2)	0.3949(3)	0.0736(7)	0.6693(3)
N(3)	0.4691(2)	−0.1233(5)	0.6710(3)
C(4)	0.4321(3)	−0.2655(7)	0.5860(3)
C(5)	0.3150(3)	−0.1871(7)	0.5250(3)
C(6)	0.3714(3)	0.1642(7)	0.7834(3)
C(7)	0.3416(4)	−0.0265(9)	0.8610(3)
C(8)	0.4786(4)	0.293(1)	0.8409(4)
C(9)	0.2669(4)	0.3248(8)	0.7620(3)
C(10)	0.5932(3)	−0.1210(9)	0.7228(4)
O(11)	0.4851(2)	−0.4323(5)	0.5616(2)
C(12)	0.0685(3)	0.4699(7)	0.2359(3)
C(13)	0.1194(4)	0.6778(7)	0.2289(3)
C(14)	0.1721(4)	0.7325(8)	0.1334(4)
C(15)	0.1705(4)	0.585(1)	0.0464(3)
C(16)	0.1187(4)	0.3800(9)	0.0527(3)
C(17)	0.0680(4)	0.3234(8)	0.1474(3)
C(18)	0.0157(3)	0.4074(7)	0.3401(3)
O(19)	−0.0957(2)	0.3001(6)	0.3084(2)
C(20)	0.0950(3)	0.2458(7)	0.4156(3)
O(21)	0.1929(2)	0.3163(5)	0.4653(2)
O(22)	0.0581(2)	0.0521(5)	0.4219(2)

Table 8 Fractional co-ordinates for BMI-*S*-MA with e.s.d.s in parentheses

Atom	*x*/a	*y*/b	*z*/c
N(1)	0.8847(5)	0.5556	0.1655(4)
C(2)	1.0190(6)	0.648(1)	0.2253(5)
N(3)	1.0875(5)	0.569(1)	0.1588(4)
C(4)	1.0047(7)	0.512(1)	0.0565(5)
C(5)	0.8720(6)	0.506(1)	0.0535(5)
C(6)	1.0735(6)	0.572(1)	0.3469(5)
C(7)	1.1115(7)	0.328(2)	0.3572(6)
C(8)	1.1905(9)	0.719(2)	0.4094(7)
C(9)	0.9662(7)	0.614(2)	0.3918(5)
C(10)	1.2194(7)	0.633(2)	0.1789(6)
O(11)	1.0397(5)	0.479(1)	−0.0201(4)
C(12)	0.5587(6)	0.248(1)	0.2149(5)
C(13)	0.5891(7)	0.449(1)	0.2720(6)
C(14)	0.5548(7)	0.483(2)	0.3608(6)
C(15)	0.4871(7)	0.324(2)	0.3909(6)
C(16)	0.4546(7)	0.122(2)	0.3330(6)
C(17)	0.4897(7)	0.088(2)	0.2446(6)
C(18)	0.6047(6)	0.211(1)	0.1199(5)
O(19)	0.5024(5)	0.118(1)	0.0290(4)
C(20)	0.7165(6)	0.051(1)	0.1578(4)
O(21)	0.8242(4)	0.129(1)	0.2145(4)
O(22)	0.6964(4)	−0.1561(9)	0.1340(4)

lizing from absolute ethanol. $[\alpha]_D = -89°$ (*c* 1 EtOH); elemental analysis and IR spectrum were identical to the data published in ref. 10.

(R)-2-tert-*Butyl*-3-*methyl*-4-*oxoimidazolidinium* (S)-*mandelate*. After filtering off BMI-*R*-MA, the mother liquor contained BMI-*S*-MA in high optical purity (89%). It was obtained by evaporating the solvent. $[\alpha]_D = 44°$ (*c* 1 in EtOH) (0.76 g, 99% of the theoretical amount of the BMI-*S*-MA) (Found: C, 62.0; H, 7.8; N, 9.0. Calc. for $C_{16}H_{24}N_2O_4$: C, 62.3; H, 7.8; N, 9.1%). IR, see Table 5. The crude diastereoisomeric salts were subject to decomposition.

(R)- *and* (S)-*mandelic acid*. The appropriate BMI-MA salt was dissolved in minimum amount of water. pH was adjusted to 1, and the liberated mandelic acid extracted three times with diethyl ether. On evaporating the solvent from the combined extracts, optically active mandelic acid was obtained with a yield of *ca.* 90%, calculated from the starting diastereoisomeric salt. $[\alpha]_D = 152 \pm 2°$ (*c* 1 in EtOH). Recrystallization of the sample from a minimum amount of concentrated aqueous HCl provided enantiopure species: $[\alpha]_D = 156°$ (*c* 1 in EtOH).

Suitable single crystals were obtained by recrystallizing the crude salts from diethyl ether at 40 °C for BMI-*R*-MA and 5 °C for BMI-*S*-MA.

Acknowledgements

The authors are grateful to Professor D. Seebach (ETH-Zurich) for his interest, support and stimulating discussions, and to Professor E. Fogassy (Technical University Budapest) for his comments on the MS.

References

1 S. H. Wilen, A. Collet and J. Jacques, *Tetrahedron*, 1977, **33**, 2725.
2 E. Fogassy, F. Faigl and M. Ács, *Tetrahedron*, 1985, **41**, 2837.
3 S. H. Wilen, *Tables of Resolving Agents and Optical Resolutions*, ed. E. Eliel, University of Notre Dame Press, Notre Dame, Ind., London, 1972.
4 P. Newman, *Optical Resolution Procedures for Chemical Compounds*, vols. 1–3, Optical Resolution Information Center, Manhattan College, Riverdale, New York, 1978–1984.
5 E. Fogassy, M. Ács, F. Faigl, K. Simon, J. Rohonczy and Z. Ecsery, *J. Chem. Soc., Perkin Trans. 2*, 1986, 1881.
6 R. O. Gould and M. D. Walkinshaw, *J. Am. Chem. Soc.*, 1984, **106**, 7840; F. Toda and H. Tanaka, *Tetrahedron Lett.*, 1981, **22**, 4669.
7 R. O. Gould, R. Kelly and M. D. Walkinshaw, *J. Chem. Soc., Perkin Trans. 2*, 1985, 847.
8 M. Czugler, I. Csöregh, A. Kálmán, F. Faigl and M. Ács, *J. Mol. Struct.*, 1989, **196**, 157; M.-C. Brianso, *Acta Crystallogr., Sect. B*, 1976, **32**, 3040; 1978, **34**, 679; M-C. Brianso, M. Leclercq and J. Jacques, *Acta Crystallogr., Sect. B*, 1979, **35**, 2751.
9 G. L. Silvey, Ph.D. Thesis, Duke University, 1984.
10 R. Fitzi and D. Seebach, *Angew. Chem.*, 1986, **98**, 363.
11 E. Fogassy, A. Lopata, F. Faigl, F. Darvas, M. Ács and L. Toke, *Tetrahedron Lett.*, 1980, **21**, 647.
12 M. Leclercq, A. Collet and J. Jacques, *Tetrahedron*, 1976, **32**, 821.
13 D. Kozma, Gy. Pokol and M. Ács, *J. Chem. Soc., Perkin Trans. 2*, 1992, 435.
14 I. Prigogine, *Chemisches Thermodynamik*, Akademische Verlag, Berlin, 1961; J. Jacques, A. Collet and S. H. Wilen, *Enantiomers, Racemates and Resolutions*, Wiley and Sons, New York, 1981.
15 E. Dahlen, M. Hjalmarson, T. Norin, I. Csöregh and A. Ertan, *Acta Chem. Scand.*, 1991, **45**, 200.

Paper 2/03614B
Received 8*th July* 1992
Accepted 4*th August* 1992